Nanoscale spectroscopy and tomography with the HZB X-ray microscope: Applications in materials and life sciences

P Guttmann, S Rehbein, S Werner, K Henzler, B Tarek, G Schneider

Helmholtz-Zentrum Berlin für Materialien und Energie GmbH, Institute for Soft Matter and Functional Materials, Albert-Einstein-Str. 15, 12489 Berlin, Germany

E-mail: peter.guttmann@helmholtz-berlin.de

Abstract. The full-field transmission X-ray microscope at the electron storage ring BESSY II allows nanoscale spectroscopy as well as correlative fluorescence and nanoscale tomographic imaging of frozen-hydrated adherent cells. Reconstructions of tilt series permit the visualization of the sub-cellular structures in mammalian cells and plant cells. Quantitative information about package densities of cell organelles in the cytoplasm is possible. We present an overview of recent results in materials and life sciences obtained with the HZB X-ray microscope.

1. Introduction

The full-field transmission X-ray microscope (TXM) at the electron storage ring BESSY II operated by the Helmholtz-Zentrum Berlin (HZB) was installed at the undulator beamline U41-FSGM [1] in 2007. It is in full user operation since spring 2008. It was the first TXM in the soft X-ray energy range operating at an undulator source with a focusing spherical grating monochromator (FSGM) and an elliptically shaped glass capillary mirror as condenser [2]. This set-up delivers a spectral resolution which is an order of magnitude higher than for conventional TXMs using a zone plate monochromator. Therefore, nanoscale spectroscopy applications like NEXAFS investigations are feasible [3]. On the other hand with this set-up no pinhole close to the specimen is necessary. The free space for specimen rotation permits to use flat sample supports. Additionally, the partially coherent object illumination delivers an improved contrast transfer function of the microscope compared to incoherent systems [4]. The schematic optical layout and the workflow for nanoscale spectroscopy and nanoscale tomography are depicted in Fig. 1.

The spatial resolution of the HZB TXM was determined to be 11 nm (half-pitch) for 2D imaging [5]. This resolution cannot be transferred directly to the 3D resolution in nanoscale tomography which is affected by the small depth of focus of the zone plate objective. In practice, the achieved 3D resolution is about 36 nm (half-pitch) [4,6].

The sample stage is a modified CompuStage from FEI Company. Therefore, TEM holders can be used. The specimens are investigated under vacuum conditions. Depending on the application, users can choose between two different holders: A room temperature holder allows mounting either round standard EM grids with 3 mm in diameter or alternatively silicon nitrate membranes with 3.5 mm x 3.5 mm in wafer size. For biological samples a cryo high tilt holder (Gatan model 630, see Fig. 2) is employed. For this holder special rectangular grids suited for high tilt were designed: IFR-1 and HZB-2 types are shown in Fig. 2. Holy carbon films like the R2/2 coating from Quantifoil [7] turned out to be the best sample support film.

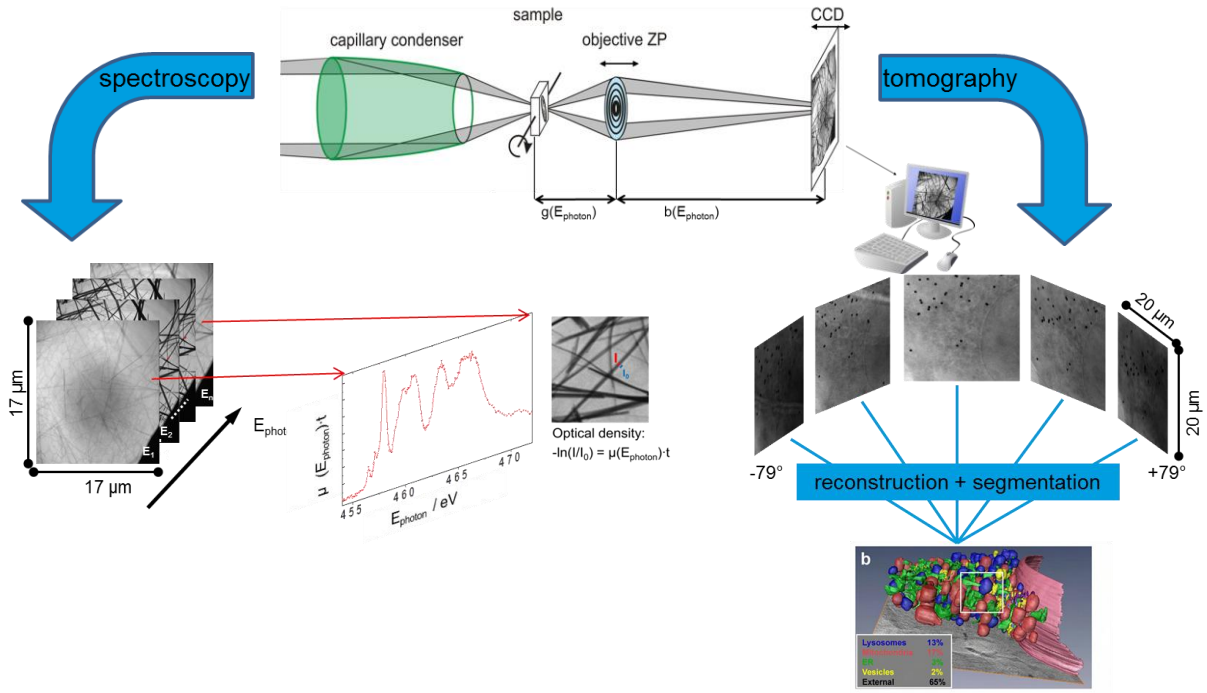

Fig. 1: Optical set-up of the HZB-TXM (upper) and workflow for nanoscale spectroscopy (lower left) and tomography (lower right) investigations.

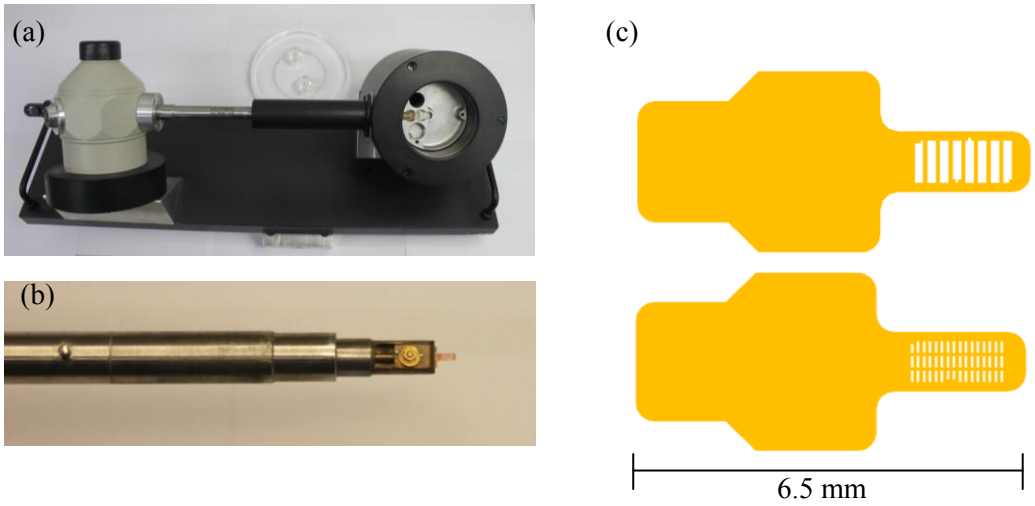

Fig. 2: The Gatan model 630 cryo high tilt holder: (a) in the transfer station, (b) showing the tip with a grid in working position. (c) Two types of high tilt grids employed for cryo tomography of cells.

Recently, a light microscope inside the X-ray microscope became accessible for users. The schematic set-up is displayed in Fig. 3. It is possible to switch between the light and the X-ray microscope working positions within 2 minutes (Fig. 4). For correlative microscopy, the sample is under the same viewing angle for light and x-ray microscopy. The light microscope delivers an overview of the samples on the grid and helps to preselect the objects without applying an X-ray dose. Additionally, the fluorescence mode can be used to identify labeled regions in cells as well as fiducial markers for correlative alignment.

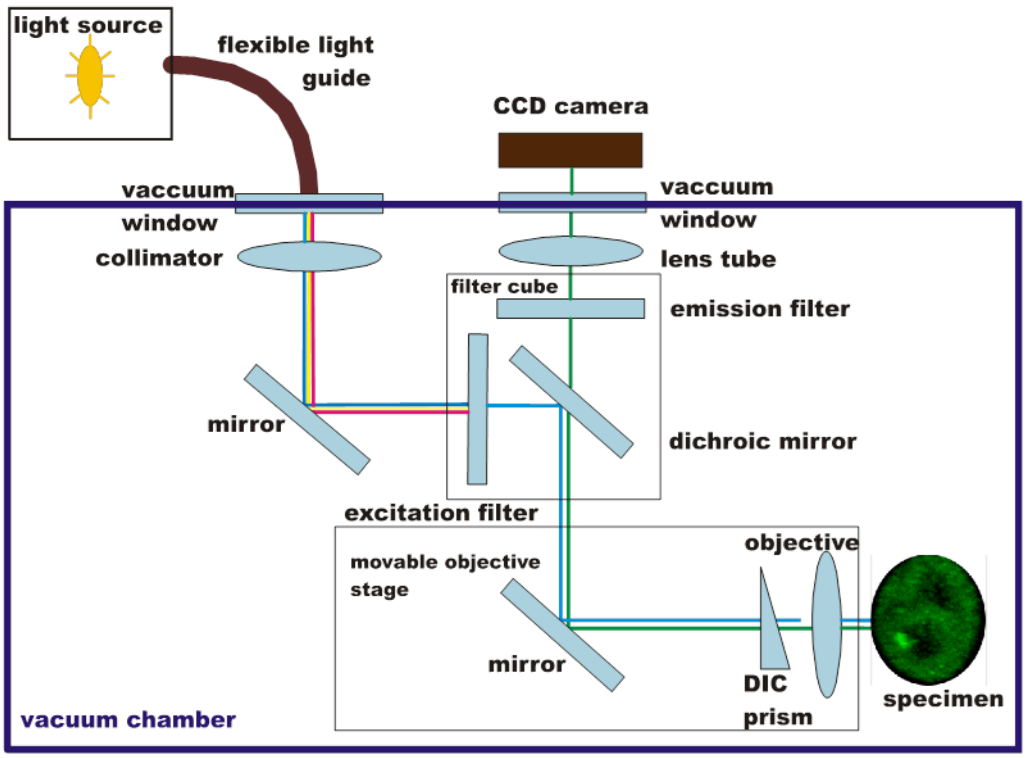

Fig. 3: Schematic layout of the incorporated light microscope. The filter cube allows switching between four different modes: bright field, differential interference contrast (DIC) and two fluorescent modes: GFP (green) and rhodamine (red). Details of the filters used in the fluorescent mode are given in Table 1.

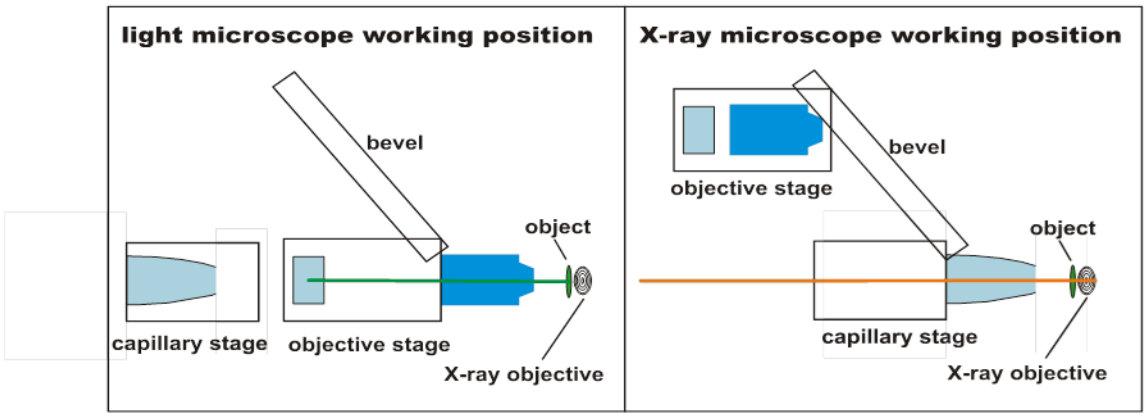

Fig. 4: Working position of the light microscope (left). Switching to the X-ray microscopy working position (right) requires to retract the light microscope objective along the optical axis with subsequent travel on the bevel to the home-position. Finally, the condenser (capillary stage) of the X-ray microscope has to be moved along the optical axis to the X-ray microscopy working position.

U41-TXM, HZB	
Microscope type	TXM
Source	Undulator beamline, linear polarization
Condenser/Objective aperture	Partially coherent illumination
Energy range	250 – 800 eV (- 1.5 keV)
Spectral resolution	up to $E/\Delta E = 10^4$
Zone plates for user operation	dr_n = 25 nm, 40 nm
Spatial resolution	2D: ≈10 nm half-period (depends on objective) 3D: ≈36 nm Rayleigh criterion
Sample format	1) Special designed rectangular grids (HZB-2 or IFR-1) having 2 mm x 1 mm sample area and open grid slits width 50 µm x 200 µm or 150 µm x 700 µm 2) 3 mm diameter EM grids or $3.5 \cdot 3.5$ mm^2 wafer, but for these no cryo and no tomography possible
Tomography capability	yes
Tilt range	-80°…. +80°
Cryo capability	yes
Detector type	Thinned, backside illuminated CCD, 1340 pixel x 1300 pixel
X-ray magnification	adjustable, value depends on the used objective
Light microscope	BF, DIC, fluorescence
Filter sets for light fluorescence microscope	Filter set 38 from Zeiss, GFP, ex 470, emm 525; Filter set 43 from Zeiss, Cy 3 (rhodamin), ex 545, emm 605
Raw data format	*.spe (WinView); 3.407 MB per image
Data analysis software capabilities available	ImageJ, Imod (eTomo)
Preparation Lab	BioLab (restricted access): safety level 2 (BioStoffV), genetically modified organisms (GMOs) belonging to safety level S1 (GenTG); incubator; plasma cleaner; plunge freezer (liquid ethane); fluorescence light microscope LEICA DMI6000B; cryo light microscopy stage (ordered)

Table 1: Main parameters of the U41-TXM and the infrastructure available for X-ray microscopy experiments at HZB.

2. Overview of the modes of operation and their applications

Two modes of operation are already outlined in Fig. 1: Nanoscale spectroscopy and tomography. The photon energy available for X-ray microscopy experiments ranges from 270 eV - 800 eV (see Table 1). Accepting a reduced photon flux, this energy range can be extended up to about 1.5 keV.

2.1. Nanoscale spectroscopy

For spectroscopy applications the CCD camera will be moved together with the objective zone plate to ensure the same image magnification at each photon energy. After collecting a data set of images, the images can be aligned using a cross-correlation method as implemented for example in the eTomo package [8] or the images can be directly imported into the aXis2000 software [9]. After the alignment, a NEXAFS spectrum for each pixel in the image can be obtained. The image field is 13 – 20 µm in square with a pixel size of 10 – 15 nm depending on the zone plate objective applied for imaging. Therefore, one image data set of nanoparticles already contains many different particles

which makes statistical analysis possible. Typically, one data set is taken within 60 – 90 minutes with a few seconds exposure time per image. Compared to scanning X-ray microscopes (SXM´s) the TXM allows a much faster data acquisition for the same amount of particles.

This mode of operation was used for the investigation of different TiO_2 nanoparticles like nanoribbons [10,11,3], carbon nanotubes, graphite layers [12] and especially synthesized microgels with TiO_2 particles [13]. Another example for using the tunability of the photon energy is the investigation of organic solar cells [14]. In most of these studies complementary methods like electron microscopy or atomic force microscopy are used to combine the findings for a more detailed interpretation.

2.2. Nanoscale tomography

Tomography studies can be performed using the high tilt grids in combination with the Gatan model 630 holder. This allows tilt angles in the range of up to ±79°. After taking a data set in typically 1° steps within about an hour with a few seconds exposure time per image, the images will be aligned. For this purpose, freely available software packages like eTomo [8] or BSoft [15] – both originally developed for electron microscopy – are used. These software packages deliver a reconstruction of the sample volume. Subsequent segmentation processes can be performed to display e.g. different organelles in cells. Besides materials sciences applications like tomography studies of stress migration in semiconductors [16] or the morphology of cement particles [17], the main application field for nanoscale tomography is cell biology. Due to the higher penetration depth of X-rays compared to electrons, tomography of whole cells in their native state is possible. Only cryo fixation without staining or sectioning is necessary to accomplish X-ray tomography studies of cells. The method of cryo fixation is well established and described for X-ray microscopy work in several publications [4,6,18-20]. Studies of mouse adenocarcinoma cells delivered already an atlas of mammalian cell ultrastructures in the cellular volume like mitochondria, nuclear membrane channels, granular structures in nucleoli and many other organelles [20].

The application of cryo X-ray tomography together with complementary methods solved the question whether the nucleation of hemazoin in the life cycle of *Plasmodium falciparum* occurs in the lipid droplet or at the lipid-water interface of the digestive vacuole. As a result it could be clearly determined that an oriented crystallization at the inner membrane in the aqueous rather than the lipid phase takes place [21].

The study of virus cell interactions is another field of interest: In a first attempt it was demonstrated that membranes and inner compartments of Vaccinia viruses could be resolved by cryo X-ray tomography [18]. In a second step these viruses could be identified in cells. Combining the use of the incorporated fluorescent light microscope together with subsequent investigations by electron microscopy, viral factories within cells could be defined and volume representations of different states of these viruses (immature and mature) were achieved [19].

Furthermore, tomography studies of cells treated with a fluorophore-tagged protein showing the same behavior as Herpes viruses show different aspects of changes within the cell nucleus [6].

Additionally, quantitative findings on the volume densities of different cell organelles within the cytoplasm of mammalian cells [3] or within e.g. algae [22] were procurable.

3. Outlook

Current nanoscale tomography studies pave the way to a better understanding of the interaction of nanoparticles with cells and help to understand their toxicological effects on cells. These investigations are important for humankind as nowadays many substances used e.g. for sun-milks or for paints contain nanoparticles. Developing new fiducial markers visible as well in the fluorescent light microscope as in the X-ray microscope will allow for correlative microscopy. So far, by default cryo samples were prepared by plunge freezing in liquid ethane or in a mixture of ethane and propane [6], but recently it was verified that high pressure freezing might be advantageous [24].

Acknowledgements
This work was funded in part by the Human Frontier Science Program Research Grant Ref. RGP0053/2005-C, the German Federal Ministry of Education and Research under contract number 05KS4BY1/7, the 7th framework program under grant agreement 226716 (WP23 NANOFOX) and BioStruct-X under grant agreement number 283570.

References

[1] G. Schneider, P. Guttmann, S. Rehbein, S. Werner, R. Follath, J. Struct. Biol. **177** (2012), 212-223
[2] P. Guttmann, X. Zeng, M. Feser, S. Heim, W. Yun, G. Schneider, Journal of Physics: Conference Series **186** (2009) 012064
[3] P. Guttmann, C. Bittencourt, S. Rehbein, P. Umek, X. Ke, G. Van Tendeloo, C.P. Ewels, G. Schneider, Nature Photonics **6** (2012), 25-29
[4] G. Schneider, P. Guttmann, S. Heim, S. Rehbein, F. Mueller, K. Nagashima, J.B. Heymann, W.G. Müller, J.G. McNally, Nature Methods **7** (2010), 985-987
[5] S. Rehbein, P. Guttmann, S. Werner, G. Schneider, Optics Express **20** (2012), 5830-5839
[6] C. Hagen, P. Guttmann, B. Klupp, S. Werner, S. Rehbein, T.C. Mettenleiter, G. Schneider, K. Grünewald, J. Struct. Biol. **177** (2012), 193-201
[7] http://www.quantifoil.com/
[8] eTomo is part of the IMOD package: http://bio3d.colorado.edu/imod/
[9] http://unicorn.mcmaster.ca/aXis2000.html
[10] C. Bittencourt, P. Krüger, M.J. Lagos, X. Ke, G. Van Tendeloo, C. Ewels, P. Umek, P. Guttmann, Beilstein J. Nanotechnol., accepted for publication
[11] P. Guttmann, C. Bittencourt, X. Ke, G. Van Tendeloo, P. Umek, D. Arcon, C.P. Ewels, S. Rehbein, S. Heim, G. Schneider, in: I. McNulty, C. Eyberger, B. Lai (Eds.), The 10th International Conference on X-ray Microscopy, AIP Conference Proceedings **1365** (2011), 437-440
[12] C. Bittencourt, A.P. Hitchock, X. Ke, G. Van Tendeloo, C.P. Ewels, P. Guttmann, Beilstein J. Nanotechnol. **3** (2012), 345-350
[13] K. Henzler, manuscript in preparation
[14] T. Mönch, P. Guttmann, M. Riede, L. Müller-Meskamp, K. Leo, manuscript in preparation
[15] http://lsbr.niams.nih.gov/bsoft/#
[16] E. Zschech, R. Huebner, D. Chumakov, O. Aubel, D. Friedrich, P. Guttmann, S. Heim, G. Schneider, J. Appl. Phys. **106**, 093711 (2009)
[17] S. Brisard, R.S. Chae, I. Bihannic, L. Michot, P. Guttmann, J. Thieme, G. Schneider, P.J.M. Monteiro, P. Levitz, American Mineralogist 97 (2012), 480-483
[18] J. Carrascosa, F.J. Chichón, E. Pereiro, M.J. Rodríguez, J.J. Fernández, M. Esteban, S. Heim, P. Guttmann, G. Schneider, J. Struct. Biol. **168** (2009), 234-239
[19] F.J. Chichón, M.J. Rodríguez, E. Pereiro, M. Chiappi, B. Perdiguero, P. Guttmann, S. Werner, S. Rehbein, G. Schneider, M. Esteban, J.L. Carrascosa, J. Struct. Biol. 177 (2012), 202-211
[20] W.G. Müller, J.B. Heymann, K. Nagashima, P. Guttmann, S. Werner, S. Rehbein, G. Schneider, J.G. McNally, J. Struct. Biol. 177 (2012), 179-192
[21] S. Kapishnikov, A. Weiner, E. Shimoni, P. Guttmann, G. Schneider, N. Dahan-Pasternak, R. Dzikowski, L. Leiserowitz, M. Elbaum, PNAS **109** (28) (2012), 11188-11193
[22] E. Hummel, P. Guttmann, S. Werner, B. Tarek, G. Schneider, M. Kunz, A.S. Frangakis, B. Westermann, submitted to PLOS One
[23] D. Drescher, P. Guttmann, T. Büchner, S. Werner, G. Laube, A. Hornemann, B. Tarek, G. Schneider, J. Kneipp, mauscript in preparation
[24] A. Weiner, S. Kapishnikov, E. Shimoni, S. Cordes, P. Guttmann, G. Schneider, M. Elbaum, J. Struct. Biol. (2012), available online 15 October 2012